Slip Localization and Dislocation Structure at Early Stages of Fatigue Damage in Austenitic Stainless Steel (316L)

A. Weidner[1*À], J. Man[2], W. Skrotzki[1], J. Polák[2]
[1]*Institute of Structural Physics, Technische Universität Dresden, Dresden, Germany;*
[2]*Institute of Physics of Materials, Academy of Science of Czech Republic, Brno, Czech Republic*

Abstract

During the last years, a clear evidence of cyclic slip localization within planar glide f.c.c. metals at early stages of fatigue damage and its evolution during fatigue life was obtained via surface observations of sharp surface slip markings using atomic force microscopy. The electron channeling contrast technique has been applied to study the internal structure ï dislocation structure. This powerful, non-destructive method allows observations of the dislocation arrangement responsible for surface markings as well to study their evolution in early stages of fatigue. First results of the development of dislocation structure in 316L in correlation with the markings produced by slip localizations are presented.

Keywords: slip localization, dislocation structure, fatigue, electron channeling contrast, 316L

1. Introduction

The localization of plastic strain is a typical feature in fatigue of crystalline material. It is accompanied by changes in the dislocation structure during cyclic deformation. The damage processes start at the sites of cyclic strain localization, usually called persistent slip bands (PSBs) and results in the formation of sharp surface slip markings (called persistent slip markings ï PSMs). PSMs consist of extrusions and intrusions, which develop on the initially flat surface at emerging PSBs. It is generally believed that surface fatigue cracks nucleate in these locations and grow in the interior of the material [1-5]. However, a detailed recent review of the theoretical models and computer simulations of surface relief evolution leading to fatigue crack initiation demonstrated only partial understanding of the subject [6]. Since fatigue crack nucleation is a direct consequence of the temporarily irreversible slip activity localized within PSBs, detailed knowledge on the slip activity and dislocation structure of PSBs and their evolution during cycling is essential for understanding the fundamental mechanisms of surface relief formation and fatigue crack initiation and for verifying the theoretical models of fatigue crack initiation.

* Corresponding author: aweidner@physik.tu-dresden.de
À since 01/01/2009 at Institute of Material Science, Technische Universität Bergakademie Freiberg. Germany weidner@ww.tu-freiberg.de

The dislocation arrangement in the matrix and PSBs as well as the resulting surface relief of PSMs is strongly affected by the character of slip. The planarity of slip in metals and alloys depends on the stacking fault energy (SFE) as well as on the short range order (SRO) of dislocations. Depending on the value of SFE, fcc metals and alloys can be divided into two groups: wavy slip metals (high SFE) and planar slip metals (low SFE) [3, 4, 7]. The cross slip of dislocations is easier for higher SFE which results in wavy slip. Further it increases the interaction between dislocations, resulting in the increase in work hardening. However, interstitials as nitrogen as alloying elements for instance in austenitic stainless steels inhibit cross slip of dislocations and promotes planar slip. It was shown that N do not influence or little lowers the SFE. Instead it was shown by [8] that the planar distribution of dislocations is attributed to a short range order zone. For recent review on wavy-to-planar-slip transition see also [9].

Considerable effort was given to map the dislocation structure in the matrix and PSBs and its evolution in order to explain the accommodation of a high cyclic plastic strain in PSBs in case of fcc metals with medium SFE, e.g. copper [2, 5, 7, 10, 11] and high SFE, e.g. nickel [12, 13]. The correlation between surface relief of an emerging PSB and its specific dislocation structure (called ladder-structure) has been established and is commonly accepted [1, 5, 14].

Experimental data concerning planar slip fcc metals offer a far less clear picture. Contrary to the clear evidence of cyclic slip localization obtained recently via surface observations of sharp surface slip markings and their evolution (see e.g. [15-19], so far there is uncertainty about the internal structure of the respective PSBs. Dislocation structures have been studied using transmission electron microscopy (TEM) mainly in the case of single crystals of Cu-Zn [7, 20] and Cu-Al [21-23] alloys. Buchinger et al. [24] found dislocation structures corresponding to localization of the cyclic plastic strain - so-called ñpersistentò Lüders bands (PLBs). But data obtained from optical interferometry [21] suggested that these PLBs are not really ñpersistentñ in the sense that they occur at the same place after re-polishing and re-loading. On the other hand, PSBs with a structure more or less reminiscent of the well-known ladder-structure were identified at the end of fatigue life of 316L [25, 26]. Recently, Kaneko et al. [27] found PSBs with ladder-structure at the half of fatigue life using electron channeling contrast (ECC). Although the ECC technique is predestinated for a systematic study of the development of dislocation structures within individual grains with respect to their crystallographic orientation, such a study has not been performed so far for planar glide metals.

Systematic atomic force microscopy (AFM) studies of Man et al. [28, 29] on surface relief evolution of 316L steel cycled with constant plastic strain amplitude has revealed very early localization of the cyclic plastic strain. PSMs corresponding to the primary slip system were detected in the majority of grains already after 10 cycles and are well developed at 1 000 cycles.

It is the aim of the present paper to show first results on the investigations of macroscopic glide localization and corresponding dislocation structures on the mesoscopic scale early in the fatigue life of polycrystalline 316L steel.

2. Experimental procedures

2.1. Material, specimens, fatigue tests

The investigations of slip localization in materials with planar glide were carried out on surface grains of polycrystalline austenitic stainless steel supplied by Uddeholm (Sweden). Its chemical composition (in wt %) is given by Table 1. Average grain size found using the line interception method neglecting twin boundaries was 40 µm.

Table 1
Chemical composition of 316L austenitic stainless steel (in wt %)

C	Mn	Si	P	S	Cr	Ni	Mo	Fe
0.018	1.68	0.42	0.015	0.001	17.6	13.8	2.6	rest

Flat specimens with a square cross section of 5 × 5 mm² and a gauge length of 8 mm were prepared by spark erosion. In order to remove stresses after machining the specimens were heat treated at 600°C for 1h in vacuum with subsequent furnace cooling. Subsequently, the specimens were carefully prepared by mechanical grinding. In order to be able to compare present results with recent investigations of Man et al. [28, 29], a calotte was prepared as shown in figure 1. The calotte was produced by grinding a circular surface area of 3 mm in diameter to a depth of about 0.4 mm.

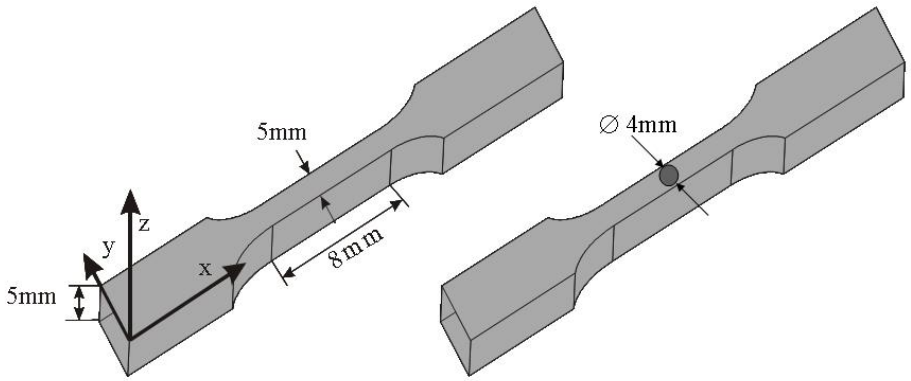

Figure 1: Specimen geometry

The cyclic deformation was carried out in a symmetric push-pull mode (R = -1) using a servo-hydraulic machine (MTS 860). The specimens were cycled at room temperature in air under plastic strain control with constant plastic strain

amplitude of $\varepsilon_{pa} = 1 \times 10^{-3}$ and a strain rate of 1.5×10^{-3} s^{-1}. The cycling was interrupted first at 1000 cycles. The specimen was removed from the testing machine for microscopic surface observation.

2.2. Microscopic observations

Microscopic observations using conventional scanning electron microscope (CSEM, Zeiss DSM 962) and field emission SEM (FESEM, Zeiss Ultra 55) were performed for surface grains to study the development of PSMs (extrusion/intrusion profile) and the developed dislocation structure. The ECC [30, 31] allows the imaging of near surface crystal defects in a bulk specimen. The contrast arises from the variation of the backscattered electron yield in strained regions of a crystal. ECC images can be taken from bulk samples making this technique very attractive for the examination of crystalline defects during in-situ deformation. ECC imaging is already well developed for the investigation of condensed dislocation structures (walls, veins, ladders) formed in fatigued materials with wavy glide slip [30]. Under special circumstances it is even possible to visualize single dislocations [31]. The CSEM is equipped with a tungsten cathode and a retractable four-quadrant back-scatter-electron (BSE)-detector. For the ECC images 25kV and an aperture of 70 µm was used. Due to the spatial arrangement of the retractable BSE-detector quite below the microscope objective pole piece, the working distance is limited to 11 mm. The FESEM is equipped with a Shottky field emission gun and a super-eucentric 6-axis (x, y, z, rotation, tilt and M) stage which allows also very precise tilting (steps of 0.1°) of the specimen. For ECC imaging 25 kV and apertures of 120µm or 240µm were used in high-current mode. This leads to probe currents of 10nA and 40nA, respectively. The BSE-detector is a four-quadrant, angular selective detector (AsB) which is directly mounted on the microscope objective pole piece. This has the advantage that the working distance can be reduced to 3-4 mm.

Special BSE imaging conditions described in detail elsewhere [32] were used to observe the extrusion/intrusion profiles. The investigations were accompanied by measurements of the crystallographic grain orientation using EBSD-technique.

The shape of the calotte used in present study was not suitable for the measurement of geometric dimensions of extrusion/intrusion profiles using AFM. Results of detailed AFM-investigation are given in Ref. [28, 29].

3. Results and discussion

3.1 Cyclic strain localization

The imaging technique described in [32] using separate sectors with opposite gains of a four-quadrant BSE-detector is especially suitable for distinguishing between slip steps on the surface and real extrusions. While slip steps at the

surface either show bright or dark contrast for opposite sectors, extrusions show a combination of bright and dark contrast for one illumination direction. The contrast completely reverses using the opposite direction. This is well demonstrated in Fig. 2 for surface grain no. 1 showing three different activated slip systems marked by three different angles with respect to the loading axis x which in all SEM micrographs lies horizontal. The upper part shows a SEM micrograph using all four quadrants of the BSE-detector. The lower part shows SEM micrographs of the same grain but with different ñilluminationò directions indicated by arrows.

Quite recently, Man et al. [28, 29] have shown by a systematic AFM study of surface relief evolution in 316L that cyclic slip localizations occur quite early in the fatigue life. Fine slip markings as well as first PSMs were already observed after 10 cycles in the majority of grains investigated. With further cycling the former fine slip markings become sites where PSMs starts to develop. PSMs are formed along the primary slip plane. Slip markings according to secondary slips systems 1 and 2 are only slip steps.

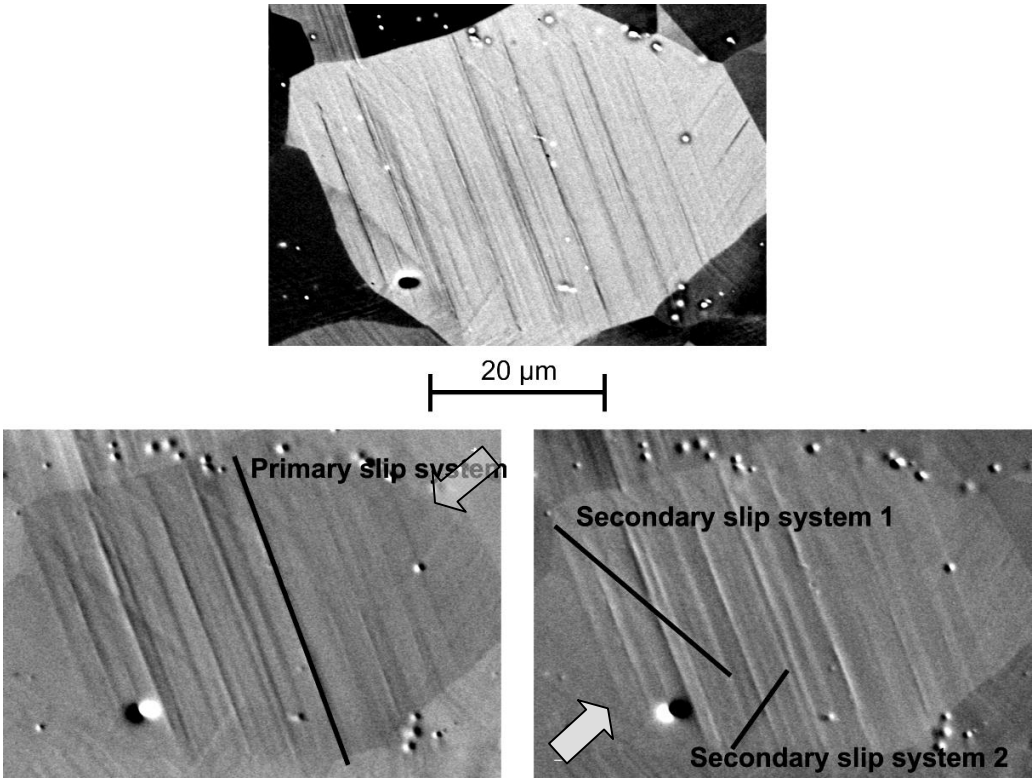

Figure 2: Appearance of extrusions and slip steps on surface grain no. 1 cycled up to N = 1000 ($\varepsilon_{pa} = 1 \times 10^{-3}$) using special BSE-imaging conditions. Different illumination directions are indicated by arrows.

It is apparent that at 1000 cycles the PSMs are already well developed. From intensive studies of fcc materials with medium to high SFE it is well known that

the cyclic slip localization is strongly correlated with a characteristic development of the dislocation structure. Therefore, it is expected that a characteristic dislocation structure can be observed in 316L steel at 1000 cycles using the ECC technique

3.2 Dislocation structure

Investigations of the dislocation structure early in the fatigue life (N = 1000) using the non-destructive ECC technique were not carried out so far. Figure 3 shows a comparison of ECC-images of the same grain as shown in Figure 2. Unfortunately, the surface after repolishing is quite rough. Images of Figs. 3(a) and (b) were taken by CSEM and FESEM, respectively. Figs. 3(c) and (d) show the marked area in (b) at higher magnification. A great difference between these two microscopes becomes apparent. It is practically impossible to image the dislocation structure using CSEM; only surface roughness (from the electro-polishing procedure) is visible. However, despite surface roughness the early evolution of the dislocation structure can be observed using the FESEM at high magnification (> 5000).

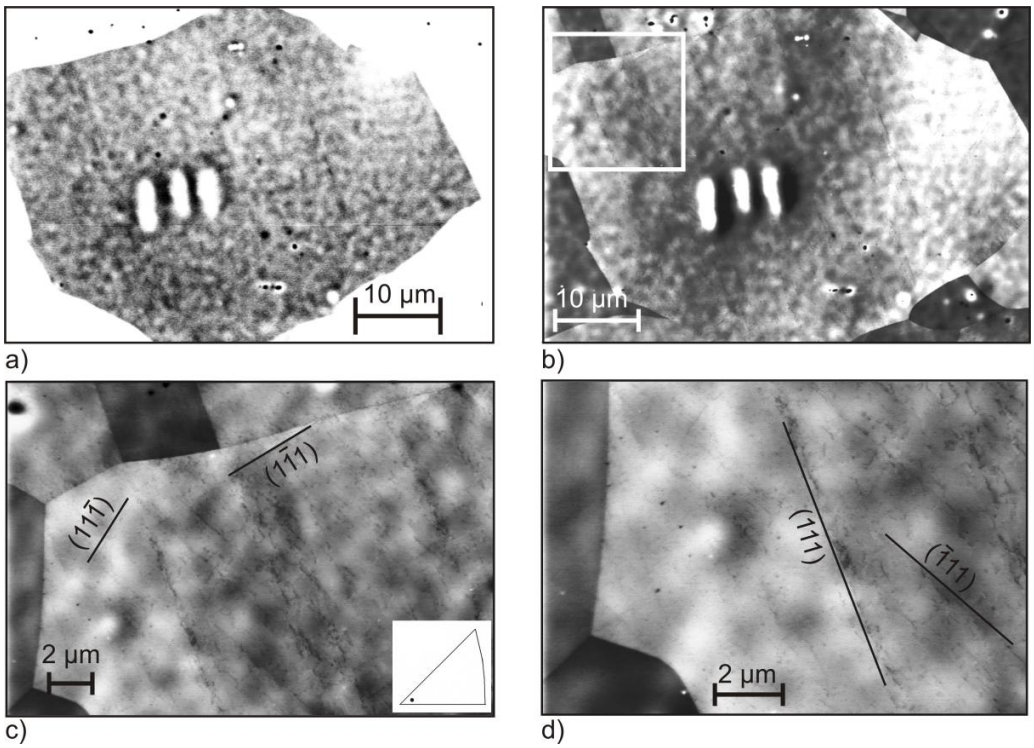

Figure 3: ECC images of an individual surface grain (no. 1) cycled up to N = 1000 ($\varepsilon_{pa} = 1 \times 10^{-3}$) which corresponds to 2.2% N_f. (a) and (b) images after repolishing the specimen surface taken by CSEM and FESEM, respectively. (c) and (d) show marked area (white rectangle) of (b) at higher magnifications with traces of slip planes indicated. The orientation of the loading axis for grain no. 1 is given by the stereographic standard triangle in (c).

It is apparent from image (d) that a planar dislocation structure starts to develop locally at 1000 cycles. Grain no. 1 with <100> parallel to the loading axis as shown by the stereographic standard triangle in (c) is oriented for multiple slip. The crystallographic data of grain no.1 regarding the active slip systems are summarized in table 2. The dislocation arrangements observed in grain no. 1 very well correspond to the traces of all four possible slip planes. Whereas primary slip takes place in the whole grain, slip on secondary systems only occurs in regions close to grain boundaries. This is in good agreement with experimental findings of other authors [33]. The pronounced PSMs (extrusions) in Fig. 2a correspond very well to the dislocation arrangement along the primary slip plane (111) in Fig.3 d). The other slip markings (SMs) (see Figure 2) which are only slip steps run parallel to secondary slip planes.

Table 2 Possible slip systems of grain no. 1. The active ones should be those with high Schmid-factors.

(111)			$(\bar{1}11)$			$(11\bar{1})$			$(1\bar{1}1)$		
μ	α	b	μ	α	b	μ	α	b	μ	α	b
0.45	-65°	$[\bar{1}01]$	0.44	-44°	$[101]$	0.42	53°	$[0\bar{1}\bar{1}]$	0.38	33°	$[011]$
0.39		$[0\bar{1}1]$	0.41		$[0\bar{1}1]$	0.36		$[\bar{1}0\bar{1}]$	0.36		$[\bar{1}01]$
0.06		$[\bar{1}10]$	0.03		$[110]$	0.05		$[1\bar{1}0]$	0.02		$[110]$

μé Schmid-factor, αé trace angle of the slip plane on the surface (x-y-plane) with respect to the loading axis x, bé Burgersvector

Up to 1000 cycles no extended walls, bundles or veins are formed. Very locally first condensation/localization of dislocations occurs as can be seen in the encircled area of figure 4 (a). This is a clear difference to wavy glide materials. For comparison figure 4 (b) illustrates the dislocation structure developed in a surface grain of pure nickel cycled up to 1000 cycles with $\varepsilon_{pa} = 5 \times 10^{-4}$. It is evident that among many fine slip markings (steps) some single extrusions are already developed. Additionally, a well developed dislocation wall structure is apparent.

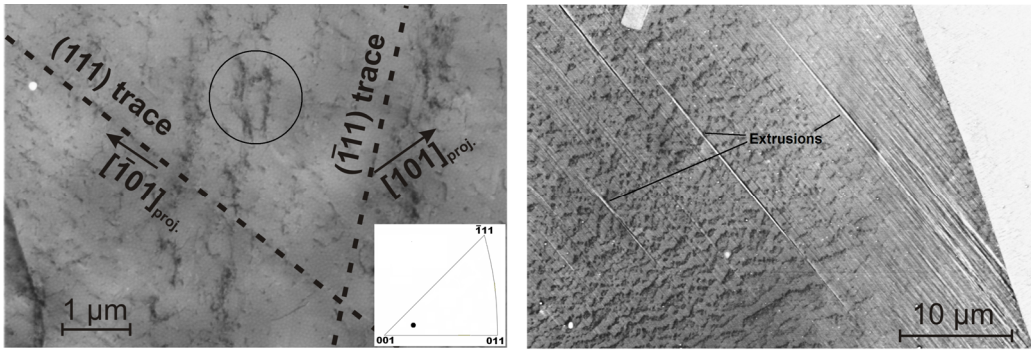

a) b)

Figure 4: High-resolution ECC-images taken by FESEM (a) Planar dislocation structure developed in surface grain no. 5 of 316L fatigued up to 1000 cycles (ε_{pa}

= 1 × 10^{-3}). The crystallographic orientation of this grain (loading axis) and the two activated slip systems are indicated. (b) Wall structure in a surface grain of pure nickel fatigued up to 1 000 cycles (ε_{pa} = 5 × 10^{-4}).

At this early stage of fatigue, the dislocation structure in 316L mainly consists of single dislocations. This becomes evident from the experimental finding that slight tilting of the specimen around the loading axis (x-axis) brings the dislocations out of contrast as shown in figure 5. Three single dislocations are marked by black arrows. At a tilt angle Θ = -1° all three dislocation are in contrast, whereas at Θ = 4° they are out of contrast.

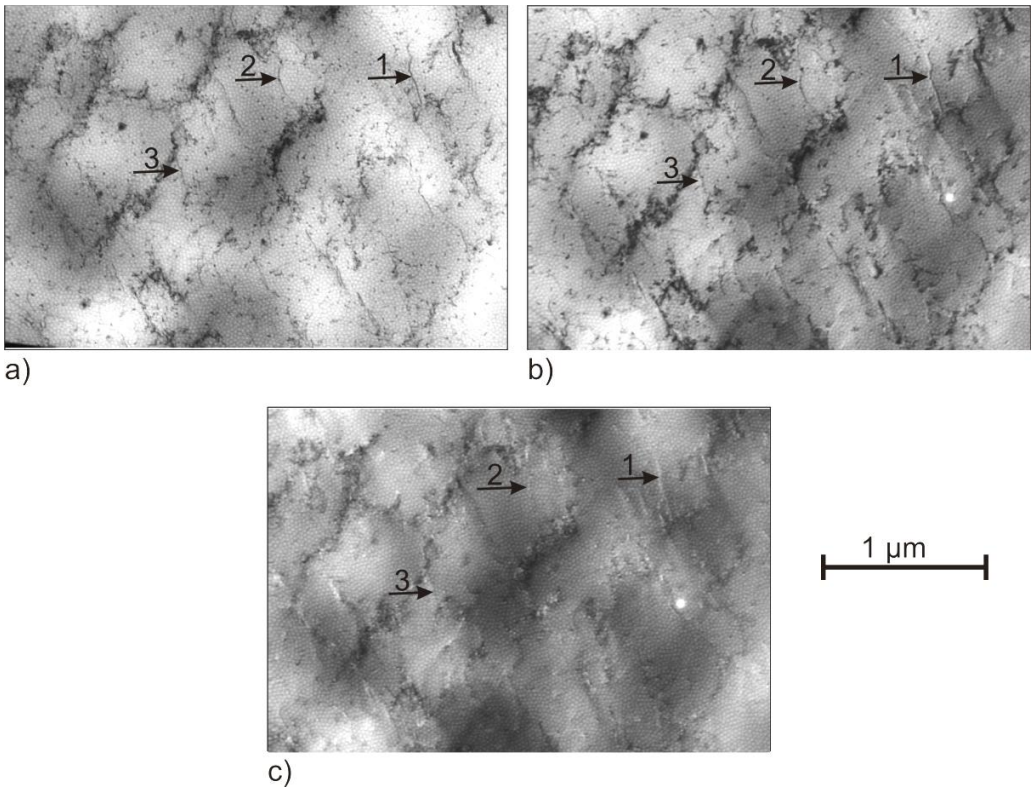

Figure 5: Planar dislocation structure within individual surface grain no. 6 of 316L cycled up to 1000 cycles (ε_{pa} = 1 × 10^{-3}) at different tilt angle Θ. (a) Θ = -1° (b) Θ = 0° (c) Θ = 4°. (FESEM)

The experimental findings are in good agreement with previous TEM results [26, 34, 35]. At this stage of fatigue life the dislocation structures developed are comparable to those in 316L single crystals which consist of planar edge dislocations arrays in the form of tangles on the primary slip plane. Locally, in particular close to grain boundaries also wall structures starts to develop which is typical for 316L polycrystals due to multiple slip [26, 34].

It should be noted that CSEM is insufficient to study the beginning evolution of planar dislocation structures at early stages in fatigue life. In contrast to the tungsten cathode, the Shottky field emission gun, due to the very small spot size (< 10nm) has a higher resolution. The resolution of ECC-images using a FESEM is comparable to dislocation structure micrographs taken by TEM. FESEM in combination with an AsB detector and large apertures offers the possibility to image the dislocation arrangement early in fatigue life and hence study its development.

5. Conclusions

The study of the slip localization and dislocation structure in early stages of fatigue damage in austenitic stainless steel (316L) can be summarized as follows:

(1) Cyclic slip localization starts to develop very early in the fatigue life at about 10 cycles. The first extrusions are well developed at 1000 cycles.
(2) At 1000 cycles planar dislocation structures start to develop. Very locally the first condensation of dislocations can be observed.
(3) CSEM is insufficient for imaging the evolution of dislocation structures at very early stages of fatigue damage by the ECC-technique.
(4) Application of FESEM leads to ECC-images resolving the planar dislocation structures.
(5) Pronounced extrusions occur in materials both with wavy glide (nickel) and with planar glide at 1000 cycles which corresponds to the onset of cyclic hardening (nickel) and cyclic softening (316L), respectively. The dislocation structures developed are different for both materials. While in nickel the typical fatigue dislocation structure is already well developed, in 316L steel the planar dislocation structure seems to begin its development.

Acknowledgement

Financial support under grants Sk 21/24-2 of Deutsche Forschungsgemeinschaft (DFG) and 106/06/1096 and 101/07/1500 of Grant Agency of Czech Republic (GACR) is grateful acknowledged.

References

[1] H. Mughrabi, in: Dislocations and Properties of Real Material, Book No. 323, The Institute of Metals, London, 1985, pp. 244ï 262.
[2] C. Laird, in: Physical Metallurgy, 4th ed., Chapter 27, R.W. Cahn and P. Haasen (eds.), Elsevier Science, 1996, pp. 2293ï 2397.
[3] S. Suresh, Fatigue of Materials, 2nd ed., Cambridge University Press, 1998.
[4] P. Lukáġ, in: Encyclopedia of Materials: Science and Technology, Vol. 3, K.H. Jürgen Buschov et al. (eds.), Elsevier Science, Oxford, 2001, pp. 2884ï 2894.
[5] J. Polák, in: Comprehensive Structural Integrity, Vol. 4, I. Milne, R.O. Ritchie and B. Karihallo (eds.), Elsevier, Amsterdam, 2003, pp. 1ï 39.

[6] J. Man, K. Obrtlík, J. Polák, Phil. Mag., submitted.
[7] M. Klesnil, P. Lukáġ, Fatigue of Metallic Materials, 2nd ed., Prague-Amsterdam, Academia-Elsevier, 1992.
[8] T. Takemoto, K. Mukaj, K. Hoshino, Transactions of the Iron and Steel Institute Japan (ISIJ) 26 (1986) 337-344.
[9] Z. Wang, Phil. Mag. 84 (2004) 351.
[10] C. Laird, P. Charsley, H. Mughrabi, Mater. Sci. Eng. 81 (1986) 433-450.
[11] Z.S. Basinski, S.J. Basinski, Prog. Mater. Sci. 36 (1992) 89-148.
[12] C. Buque, Int. J. Fatigue 23 (2001) 459-466.
[13] C. Holste, Phil. Mag. 84 (2004) 299-315.
[14] P. Lukáġ, L. Kunz, Phil. Mag. 84 (2004) 317-330.
[15] Y. Nakai, T. Kusukawa, N. Hayashi, in: Fatigue and Fracture Mechanics: 32nd Volume, ASTM STP 1406 (R. Chona, Ed.), West Conshohocken, PA, American Society for Testing and Materials, 2001, pp. 122ï 135.
[16] J. Man, K. Obrtlík, C. Blochwitz, J. Polák, Acta Mater. 50 (2002) 3767-3780.
[17] P. Villechaise, L. Sabatier, J.C. Girard, Mater. Sci. Eng. A323 (2002) 377-385.
[18] J. Man, K. Obrtlík, J. Polák, Mater. Sci. Eng. A351 (2003) 123-132.
[19] J. Polák, J. Man, K. Obrtlík, Mater. Sci. Forum 482 (2005) 45-50.
[20] P. Lukáġ, L. Kunz, J. Krejļí, Scripta Metall. Mater. 26 (1992) 1511-1516.
[21] B.D. Yan, A.S. Cheng, L. Buchinger, S. Stanzl, C. Laird, Mater. Sci. Eng. 80 (1986) 129-142.
[22] C. Laird, S. Stanzl, R. de la Veaux, L. Buchinger, Mater. Sci. Eng. 80 (1986) 143-154.
[23] S.I. Hong, C. Laird, H. Margolin, Z. Wang, Scripta Metall. Mater. 26 (1992) 1517-1522.
[24] L. Buchinger, A.S. Cheng, S. Stanzl, C. Laird, Mater. Sci. Eng. 80 (1986) 155-167.
[25] M. Gerland, J. Mendez, P. Violan, B. Ait-Saadi, Mater. Sci. Eng. A118 (1989) 83-95.
[26] T. Kruml, J. Polák, K. Obrtlík, S. Degallaix, Acta Mater. 45 (1997) 5145-5151.
[27] Y. Kaneko, K. Fukui, S. Hashimoto, Mater. Sci. Eng. A 400-401 (2005) 413.
[28] J. Man, P. Klapetek, K. Obrtlík, J. Polák, Proc. of the 16th European Conf. of Fracture (ECF 16), E.E. Gdoutos (ed.), CD ROM, Springer, Dordrecht, 2006.
[29] J. Man, P. Klapetek, O. Man, K. Obrtlík, J. Polák, Proc. of the 9th Inter. Fatigue Congress Atlanta (Fatigue 2006),CD ROM. Elsevier (2006) paper FT330.
[30] A. Schwab, J. Bretschneider, C. Buque, C. Blochwitz, C. Holste, Phil. Mag. Letters, 74 (1996) 449-455.
[31] B. A. Simkin, B-C. Ng, M. A. Crimp, Microscopy and Analysis (1999) 11-13.
[32] A. Weidner, C. Blochwitz, W. Skrotzki, W. Tirschler, Mater. Sci. Eng. A479 (2008) 181-190.
[33] J. Man, P. Klapetek, O. Man, A. Weidner, K. Obrtlík, J. Polák, Phil. Mag., submitted.

[34] Y. Li, C. Laird, Mater. Sci. Eng. A186 (1994) 65-103.
[35] J. Polák, M. Petrenec, J. Man, Mater. Sci. Eng. A400-401 (2005) 405-408.